Int. J. Heat Mass Transfer. Vol. 3, pp. 198–221. Pergamon Press 1961. Printed in Great Britain.

A REVIEW OF BINARY LAMINAR BOUNDARY LAYER CHARACTERISTICS†

J. F. GROSS, J. P. HARTNETT,‡ D. J. MASSON and CARL GAZLEY, JR.
The RAND Corporation, Santa Monica, California

(*Received* 4 *April* 1960)

Abstract—Available analyses of the binary laminar boundary layer are examined in some detail. It is demonstrated that the exact predictions of heat transfer and skin friction in the presence of mass-transfer cooling with a foreign gas can be approximated by simple expressions which should be of value for engineering design calculations.

Résumé—Les principales études de couche limite laminaire binaire sont examinées en détail. Dans cet article, on montre que les valeurs exactes du transfert de chaleur et du frottement, en présence d'un refroidissement par transport de masse à l'aide d'un autre gaz, peuvent être approchées par des relations simples qui devraient être très utiles pour les calculs des projets.

Zusammenfassung—Verschiedene Untersuchungen binärer laminarer Grenzschichten werden eingehend geprüft. Es zeigt sich, dass die exakte Berechnung des Wärmeübergangs und der Oberflächenreibung bei der Stoffübergangskühlung mit einem Fremdgas durch einfache Ausdrücke angenähert werden kann. Das ist für die techcnishe Berechnung von Auslegungsdaten von Bedeutung.

Аннотация—В статье приводится анализ бинарного ламинарного пограничного слоя. На основании проведенного анализа даётся простой и достаточно точный для инженерной практики приближенный метод расчёта теплообмена и поверхностного трения для случая охлаждения тел путём подачи в пограничный слой инородного газа.

NOMENCLATURE

c_p, specific heat at constant pressure;
c_v, specific heat at constant volume;
c_f, local skin friction coefficient, $\tau_w/\frac{1}{2}\rho_e u_e^2$;
c_{f_0}, local skin friction coefficient evaluated for solid wall exposed to same free stream conditions and held at same temperature as the actual wall;
c_H, local heat transfer Stanton number, $q/\rho_e u_e c_{p_r}(T_r - T_w)$;
c_{H0}, local Stanton number evaluated for solid wall exposed to same free stream conditions and held at same temperature as the actual wall;
c_M, mass transfer Stanton number, $\dot{m}/\rho_e u_e Y_w$;
C, Chapman–Rubesin parameter defined in equation (17);
D_{12}, ordinary diffusion coefficient;
f, dimensionless stream function;
H, enthalpy associated with change of phase;
h, heat-transfer coefficient, equation (19);
k, thermal conductivity;
m, refers to wedge flows, where free stream velocity, u_e, varies as x^m;
m_1, molecular weight of coolant gas;
m_2, molecular weight of pure air;
$\dot{m}_x$, mass flow rate of coolant gas at position x along the surface;
p, pressure;
p_1, partial pressure of coolant gas;
q, local heat-transfer rate per unit area, $k_w(\partial T/\partial y)_w$;
q_0, local heat-transfer rate per unit area evaluated for solid wall exposed to same free stream conditions and held at same temperature as actual wall;

† A condensed version of this paper was presented at the Conference on Heat and Mass Transfer, B.S.S.R. Academy of Sciences, Minsk, 5–9 June, 1961.

‡ Consultant, The RAND Corporation and Professor, Department of Mechanical Engineering University of Minnesota.

r, recovery factor;
R, universal gas constant;
T, temperature;
T^*, reference temperature defined in equation (9);
T_r, recovery temperature, defined as the wall temperature where $k_w(\partial T/\partial y)_w = 0$;
u, v, component of velocity parallel and normal to surface, respectively;
x, y, co-ordinates along and normal to the body, respectively;
Y, mass fraction of coolant gas.

Greek symbols

ρ, density;
μ, dynamic viscosity;
η, transformed co-ordinate defined in text;
ψ, stream function;
θ, dimensionless temperature;
Φ, dimension mass fraction;
λ, defined in equation (17);
ν, kinematic viscosity;
γ, ratio of specific heats, c_p/c_v;
τ_w, local shearing stress.

Dimensionless numbers

M, Mach number, ratio of local speed to local speed of sound;
Pr, Prandtl number, $\mu c_p/k$;
Sc, Schmidt number, ν/D_{12};
Re_x, local Reynolds number, $u_e x/\nu_e$.

Subscripts

1, refers to pure coolant;
2, refers to pure air;
e, evaluated at outer edge of the boundary layer;
r, refers to recovery conditions, i.e. where $k_w(\partial T/\partial y)_w = 0$;
w, evaluated at wall conditions;
x, refers to local conditions.

Superscripts

*, evaluated at the reference temperature, equation (9).

1. INTRODUCTION

RECENTLY, the alleviation of the high heating rates encountered by surfaces of hypersonic vehicles has been recognized as an important problem. One of the cooling methods that appears to have great ultimate promise is mass-transfer cooling, wherein a "foreign" material is transferred from the surface into the boundary layer. This has a two-fold advantage in alleviation of the heat-transfer problem. The transferred coolant may absorb heat from the boundary layer through a phase change (sublimation, evaporation, melting, etc.) and/or by acting as a dispersed heat sink. It will be advantageous, therefore, to employ coolants with high heats of sublimation (or evaporation, melting, etc.) as well as high thermal heat capacities. In addition, it has been shown that the introduction of a material (with its normal velocity component) at the surface acts to decelerate the flow and consequently, to reduce the skin friction. This also implies a reduction in heat transfer at the wall.

The usual boundary-layer equations are complicated by the appearance of (a) an equation defining the conservation of the species at any point in the boundary layer, and (b) transport terms which result from thermodynamic coupling coefficients such as thermal diffusion coefficient, etc. There are a number of methods for effecting the injection of a foreign material into the boundary layer, and the following descriptions have been advanced to describe specific mass-transfer cooling schemes:

(1) Transpiration cooling.
(2) Film cooling
  (a) using liquid as a coolant
  (b) using gas as a coolant.
(3) Ablation
  (a) sublimation
  (b) other ablation phenomena, such as melting, erosion, fusion, etc.

These schemes are diagrammatically shown on Fig. 1 [1].† With the exception of film cooling with a gas, these methods all involve the same mechanism in the gaseous phase of the boundary layer. However, there is a difference in the boundary conditions at the wall which distinguish the three methods from a thermodynamic as well as a mechanical viewpoint. Transpiration cooling involves the introduction of a coolant gas through a porous surface. Consequently, the rate of fluid injection through the surface and

† Figures in square brackets refer to references presented at the end of text.

into the boundary layer may be arbitrarily adjusted by purely mechanical means and the temperature at the surface may thereby be regulated depending upon the injection rate and storage temperature of the coolant gas. It should be noted that a transpiration-cooling system requires pumps, storage tanks, pressure regulators and accessory plumbing. In addition, the fabrication and maintenance of porous surfaces represents a difficult engineering problem.

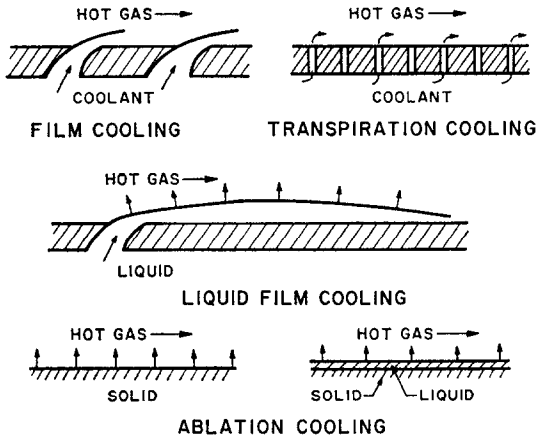

FIG. 1. Various cooling methods.

A film-cooling system involves pumping a liquid or gas on to the surface through an inlet slot configuration such that a thin film of the material covers the surface. This acts as an insulating coating and, in the case of a liquid, absorbs heat by vaporization. These systems are usually limited by such characteristics as the stability of the liquid film and the pumping power available. Film-cooling systems require essentially all the plumbing and control equipment of a transpiration-cooled operation; however, the surface construction is mechanically simpler.

A sublimation-cooling system is self-controlled through the relation between the vapor pressure and surface temperature of a solid, the Clausius–Clapeyron equation:

$$\ln p_1 = \frac{-\Delta H_s}{RT} + B \qquad (1)$$

where

p_1 = vapor pressure of subliming material,
R = universal gas constant,
H_s = heat of sublimation per mole,
B = constant of integration.

Heat is absorbed by the material as it sublimes. Thus, the heat transfer into the interior is reduced in two ways: (a) direct absorption in the form of heat of sublimation, and (b) reduction of heat transfer because of the movement of the sublimed mass away from the surface. The mass release at the surface depends upon the heat of sublimation and the temperature of the surface. Furthermore, the surface temperature can no longer be arbitrarily controlled and, in fact, will always find "its own level" depending upon the heat load, heat sublimation, and the external flow situation. It should be noted that film cooling with a liquid is essentially a sublimation process provided that the surface is completely covered by a liquid layer.

In addition to sublimation, more complex ablation cooling schemes may be visualized. Depending upon the surface material and the flight conditions, it is possible to have such phenomena as fusion of the surface material, mechanical erosion, dissociation of both air and surface material, ionization, and chemical reactions between the components in the boundary layer. The obvious complications involved in an analysis of these complex ablating systems have prevented any really accurate description of the mechanism.

There is another method of classifying these systems which may be helpful conceptually—by specifying the method of controlling the rate of injection. In the case of transpiration cooling, as we have seen, the rate is arbitrarily controlled depending upon certain mechanical requirements such as the porous surface and pumping power available. This may be considered an arbitrarily-controlled system. For a subliming or ablating surface, however, the rate of injection is determined by the heat of sublimation and the surface temperature. For a set of flight conditions and a surface material, the steady-state injection is fixed thermodynamically. We may call this a self-controlled system. Film cooling

may be considered a mixed system, with the rate of mass transfer into the boundary layer being self-controlled, but the flow rate of liquid or gas over the surface remaining arbitrary.

2. BINARY LAMINAR BOUNDARY-LAYER THEORY

Baron [2, 3], Eckert *et al.* [4–6], Sziklas and Banas [7] and Gross [8] have investigated theoretically the problem of mass-transfer cooling in the laminar boundary layer on a flat plate. The introduction of a species conservation equation as well as the appearance of thermodynamic coupling terms in both the species and energy equations complicates the mathematical analysis of the boundary layer.

The equations have been derived by Hall [9] who first treats the multicomponent fluid system and then from an order-of-magnitude argument obtains the boundary-layer equations for a binary boundary layer. The final binary boundary-layer equations for flow over a flat plate, neglecting the effects of thermal diffusion may be reproduced as follows:

Continuity:

$$\frac{\partial}{\partial x}(\rho u) + \frac{\partial}{\partial y}(\rho v) = 0. \tag{2}$$

Momentum:

$$\rho u \frac{\partial u}{\partial x} + \rho v \frac{\partial u}{\partial y} = \frac{\partial}{\partial y}\left(\mu \frac{\partial u}{\partial y}\right). \tag{3}$$

Energy:

$$\rho c_p u \frac{\partial T}{\partial x} + \rho c_p v \frac{\partial T}{\partial y} = \frac{\partial}{\partial y}\left(k \frac{\partial T}{\partial y}\right) + \mu \left(\frac{\partial u}{\partial y}\right)^2 + \rho D_{12}(c_{p_1} - c_{p_2}) \frac{\partial T}{\partial y} \frac{\partial Y}{\partial y}. \tag{4}$$

Species:

$$\rho u \frac{\partial Y}{\partial y} + \rho v \frac{\partial Y}{\partial y} = \frac{\partial}{\partial y}\left[\rho D_{12} \frac{\partial Y}{\partial y}\right]. \tag{5}$$

The boundary conditions for this system of equations follow from physical considerations:

$$\left.\begin{aligned} u &= 0 \\ T &= T_w \\ Y &= Y_w \end{aligned}\right\} \text{ at } y = 0 \tag{6}$$

$$\left.\begin{aligned} u &= u_e \\ T &= T_e \\ Y &= 0 \end{aligned}\right\} \text{ at } y \to \infty. \tag{7}$$

Since we are concerned with a seventh-order system of equations, another boundary condition must be specified. This condition may be obtained by noting that the mass velocity of the air molecules disappears at the surface of the plate; that is to say, there is no net mass transfer of the boundary layer air into the plate surface. Therefore, the mass flow of air by convection away from the surface must be equal and opposite to the diffusive flow of air toward the surface. This consideration yields the following boundary condition:

$$v = -\frac{\rho D_{12}}{1 - Y} \frac{\partial Y}{\partial y} \text{ at } y = 0. \tag{8}$$

This system of equations (2–8), forms the starting point for the various investigators cited above. In all cases, a transformation of the coordinates is next introduced with the result that the system of partial differential equations is changed into a new set of interdependent ordinary differential equations. This system of equations is still difficult to solve since, in general, all of the physical properties are functions of the local temperature and concentration of the particular gas mixtures being investigated. To obtain a representative number of solutions in a reasonable time requires the use of high speed electronic computers. Although the same basic system of differential equations was used by the various investigators (equations 2–8), somewhat different assumptions were imposed to obtain the final solution. A brief review of the available analyses is given below.

3. REVIEW OF AVAILABLE BINARY LAMINAR BOUNDARY-LAYER ANALYSES

Constant property analysis [10]

Considerable insight into the mass-transfer cooling process is obtained if it is assumed that the injected coolant has physical properties not markedly different from those of the main stream, thereby permitting the assumption of constant physical properties. The advantage of such a constant property solution is that the dimensionless heat transfer and skin-friction

results are dependent on a minimum number of parameters. This is indicated in Figs. 2 and 3 which compare the dimensionless quantities which are of importance for the solid-wall, heat-transfer case and those arising in the presence of mass transfer. For the solid wall, it has been demonstrated [11, 12] that the constant property solutions for the dimensionless skin friction, Nusselt number and recovery factor have additional value in that they may be used even when large

$$q = -k_w \left(\frac{\partial T}{\partial y}\right)_w$$

For given free stream conditions

$$T_w = T_r \text{ when } -k_w \left(\frac{\partial T}{\partial y}\right)_w = 0$$

$$T_r = T_r(M_e, T_e)$$

Definition of heat transfer coefficient, h

$$q = h(T_w - T_r)$$

$$Nu_x = \frac{hx}{k}$$

$$\frac{Nu_x}{\sqrt{(Re_x)}} = f(M_e, T_e, T_w)$$

$$\text{Constant properties, } \frac{Nu_x}{\sqrt{(Re_x)}} = f(Pr)$$

$$T_r = T_r(Pr)$$

FIG. 2. Flat plate: solid wall, no mass transfer.

variations in physical properties are encountered (including dissociation), provided the properties are evaluated at a so-called reference temperature, T^*, which may be given explicitly in terms of the surface, the free stream and the recovery temperatures:

$$T^* = T_e + 0{\cdot}5\,(T_w - T_e) + 0{\cdot}22\,(T_r - T_e). \quad (9)$$

It will be demonstrated this temperature, T^*, will also prove of value in correlating the mass transfer results.

It should be noted from Fig. 3 that the heat transfer, q, is defined in terms of the temperature gradient at the wall. This definition is convenient in that this quantity, q, represents the convective

$$q = -k_w \left(\frac{\partial T}{\partial y}\right)_w$$

For given free stream conditions

$$T_w = T_r \text{ when } -k_w \left(\frac{\partial T}{\partial y}\right)_w = 0$$

$$T_r = T_r\left(M_e, T_e, \frac{\rho_w v_w}{\rho_e u_e}\sqrt{(Re_x)}, \text{injected gas}\right)$$

Definition of heat transfer coefficient, h

$$q = h\,(T_w - T_r)$$

$$Nu_x = \frac{hx}{k}$$

$$\frac{Nu_x}{\sqrt{(Re_x)}} = f\left(M_e, T_e, T_w, \frac{\rho_w v_w}{\rho_e u_e}\sqrt{(Re_x)}, \text{injected gas}\right)$$

$$\text{Constant properties, } \frac{Nu}{\sqrt{(Re_x)}} = f\left(\frac{\rho_w v_w}{\rho_e u_e}\sqrt{(Re_x)}, Pr\right)$$

$$T_r = T_r\left(\frac{\rho_w v_w}{\rho_e u_e}\sqrt{(Re_x)}, Pr\right)$$

FIG. 3. Flat plate: mass transfer.

heat transferred to the surface from the boundary layer, and in this sense the boundary-layer heat transfer is considered separately from the enthalpy carried across the surface by the coolant. To be consistent with this point of view, the recovery temperature, T_r, is defined as that temperature where the wall-temperature gradient vanishes; in this case there still exists a transport of enthalpy across the surface, by virtue of the coolant flow, but there is no convective heat transferred to the wall from the boundary layer.

Returning to the solutions of equations (2–8) it is obvious that the energy equation is linear and consequently, the general solution of the complete equation may be obtained from the addition of (a) a general solution of the homogeneous equation (that is, neglecting the dissipation term) and (b) a particular solution of the complete equation. The particular solution results in the specification of the recovery factor, a direct measure of the temperature assumed by the surface if it is allowed to come to equilibrium with the surroundings by convection alone.

We need, therefore, only to direct our attention to the general solution of the homogeneous equation. To accomplish this solution, a stream function, ψ, is first introduced to satisfy the continuity equation, and a new independent variable, η, and the new dependent variables defined below are substituted into the original equations:

Stream function:

$$u = \frac{\partial \psi}{\partial y}, \quad v = -\frac{\partial \psi}{\partial x} \tag{10}$$

$$\left.\begin{aligned} f &= \psi/\sqrt{(\nu u_e x)} \\ \eta &= (y/x)\sqrt{(u_e x/\nu)} \\ \theta &= (T - T_w)/(T_e - T_w) \\ \phi &= (Y_w - Y)/Y_w \end{aligned}\right\} \tag{11}$$

The following equations result:

Momentum:

$$\frac{d^3 f}{d\eta^3} + \tfrac{1}{2} f \frac{d^2 f}{d\eta^2} = 0. \tag{12}$$

Energy:

$$\frac{d^2 \theta}{d\eta^2} + \tfrac{1}{2} Pr\, f \frac{d\theta}{d\eta} = 0. \tag{13}$$

Diffusion:

$$\frac{d^2 \phi}{d\eta^2} + \tfrac{1}{2} Sc\, f \frac{d\phi}{d\eta} = 0. \tag{14}$$

Boundary conditions:

$$\left.\begin{aligned} \frac{df}{d\eta} &= 0 \\ \theta &= 0 \\ \phi &= 0 \\ f_w &= -2(v_w/u_e)\sqrt{(u_e x/\nu)} \end{aligned}\right\} \text{at } \eta = 0 \tag{15}$$

$$\left.\begin{aligned} \frac{df}{d\eta} &= 1 \\ \theta &= 1 \\ \phi &= 1 \end{aligned}\right\} \text{at } \eta \to \infty. \tag{16}$$

An important observation common to all flat-plate binary laminar boundary-layer solutions is that the mass transfer into the boundary layer must vary as $1/\sqrt{x}$ if we are to arrive at a system of ordinary differential equations. Further, we have assumed an isothermal surface and it will be shown that this is completely compatible with the imposed mass-transfer distribution.

The velocity profiles for the constant property mass-transfer system are shown in Fig. 4 for several different injection rates. Inspection of these profiles brings out the following conclusions:

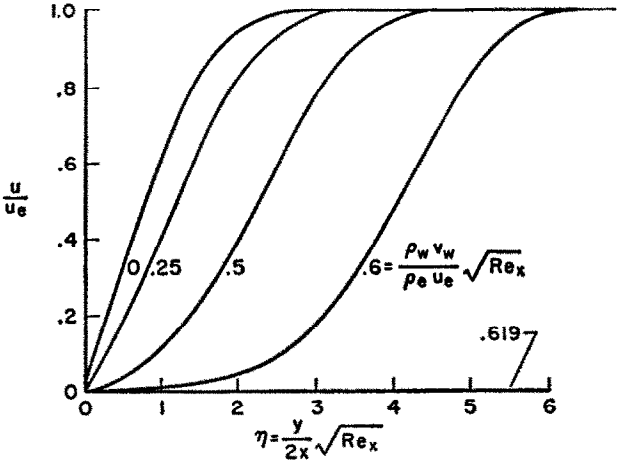

FIG. 4. Effect of air injection on velocity profile: flat plate–constant properties: laminar flow.

(a) The effect of mass addition is to thicken the velocity boundary layer.
(b) The velocity profile becomes S-shaped with mass addition, and since this is known to be an unstable type of profile, it may be concluded that mass transfer is destabilizing.
(c) The boundary layer "lifts off" the wall at a relatively low value of mass transfer; i.e. at $(\rho_w v_w/\rho_e u_e)\sqrt{(u_e x/\nu)} = 0{\cdot}619$. Apparently the boundary-layer equations fail to describe the flow field at this mass transfer condition.

The skin friction coefficient and Nusselt number, presented in Figs. 5 and 6, are seen to decrease with increasing mass transfer, both going to zero at the limiting value where the

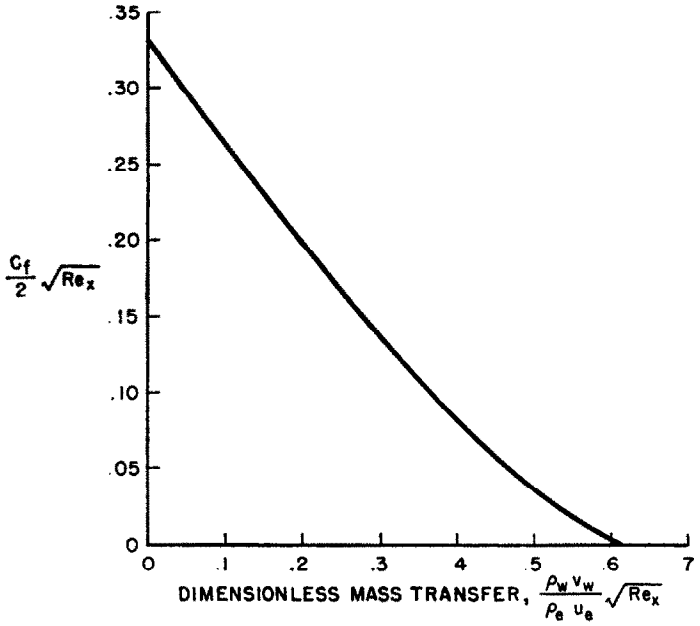

FIG. 5. Effect of air injection on local skin friction: flat plate–constant properties: laminar flow.

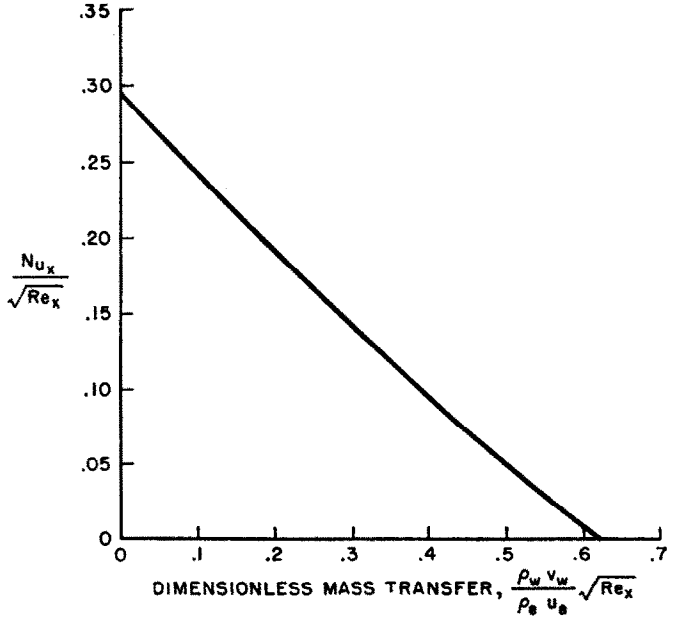

FIG. 6. Effect of air injection on local Nusselt number: flat plate–constant properties–$Pr = 0{\cdot}7$ constant wall temperature: laminar flow.

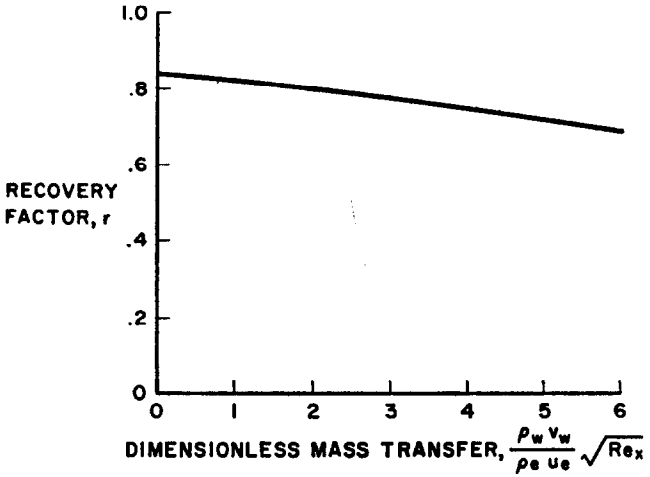

FIG. 7. Effect of air injection on recovery factor: flat plate–constant properties–$Pr = 0{\cdot}7$: laminar flow.

boundary layer "leaves" the wall. The recovery factor, shown in Fig. 7, is somewhat reduced by mass transfer but not as markedly as the Nusselt values. At hypersonic velocities the actual heat transfer to the surface is proportional to the product of the Nusselt number and the recovery temperature, and we conclude that a considerable reduction in heat transfer is obtainable with modest amounts of coolant. This is the feature which has drawn attention to this cooling scheme.

It may be noted that the heat-transfer solutions reveal that the local heat rate, q_x, is proportional to $1/\sqrt{x}$, which is precisely the distribution of the injected coolant. A simple heat balance on a sublimation or transpiration system yields the following expression.

$$\dot{m}_x[\Delta H + c_{p_1}(T_w - T_i)] = q_x$$

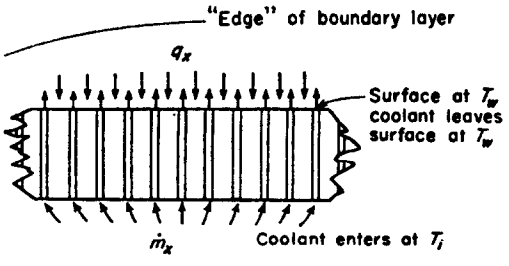

where

$\dot{m}_x$ —mass flow rate of coolant,

ΔH—change in enthalpy due to phase change,

c_{p_1} —specific heat of the pure coolant.

Thus for the situation where the coolant enters the wall at a constant temperature, T_i, or if the surface is subliming, the resulting wall temperature must be a constant. We have, therefore, demonstrated the consistency of the assumed boundary conditions.

It may be of interest to investigate the validity of the modified Reynolds analogy (which holds for solid-wall conditions) under the new conditions when mass transfer is employed. If the analogy is valid, the parameter

$$(C_H Pr^{2/3}) \div (C_f/2)$$

would equal unity. As seen in Fig. 8, the departure from unity is not significant at low mass transfer rates, with the analogy being accurate to 15 per cent up to a dimensionless mass transfer value of 0·3; at higher mass transfer rates the use of the analogy may lead to considerable error.

Analysis of Baron [2, 3]

Baron was successful in introducing the influence of variable physical properties on mass-transfer cooling, while at the same time keeping

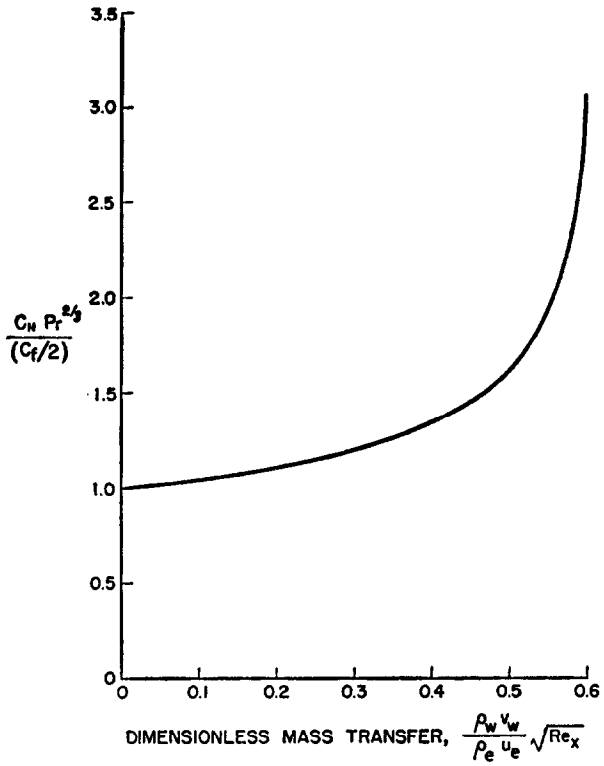

FIG. 8. Effect of mass transfer on modified Reynolds analogy: constant properties–flat plate–$Pr = 0{\cdot}7$.

the number of independent parameters at a minimum. To accomplish this, he adopted an approach similar to that used earlier by Chapman and Rubesin [13] for the solid flat plate. Baron introduces the so-called Chapman–Rubesin constant, C, for the product of the density and viscosity of the *air* only. He notes:

$$\frac{\rho\mu}{\rho_e \mu_e} = \left(\frac{\rho_2 \mu_2}{\rho_e \mu_e}\right)\left(\frac{\rho\mu}{\rho_2 \mu_2}\right) = C\lambda \qquad (17)$$

where

$C = (\rho_2 \mu_2)/(\rho_e \mu_e) =$ Chapman–Rubesin constant for *air* only

$$\lambda = \frac{\rho\mu}{\rho_2 \mu_2} = \frac{\mu}{\mu_2}\left[1 + \left(\frac{m_2}{m_1} - 1\right) Y\right]^{-1}.$$

The factor, C, is independent of the concentration, while the other factor, λ, is rigorously a function of both temperature (through μ/μ_2) and concentration. However, for helium and carbon dioxide, the gases considered by Baron, the viscosity term μ/μ_2 is relatively insensitive to temperature and is primarily dependent on the concentration.† Consequently, Baron assumes that λ is a function *only* of concentration. Using this assumption, Baron presents two approaches:

Approach 1:

Baron introduces:

$$\left.\begin{aligned} u &= \frac{\rho_e}{\rho}\frac{\partial\psi}{\partial y}, \quad v = -\frac{\rho_e}{\rho}\frac{\partial\psi}{\partial x} \\ \eta &= \frac{1}{2}\sqrt{\left(\frac{u_e}{\nu_e x C}\right)}\int_0^y \frac{\rho}{\rho_e}\,dy \\ \psi &= \sqrt{(\nu_e x u_e C)}f(\eta). \end{aligned}\right\} \qquad (18)$$

Using these transformations along with the additional assumption that the Schmidt number is a function only of concentration (an independent check shows this to be a realistic assumption), Baron obtains a set of three ordinary differential equations, similar in form but more complex than equations (12–16). The net result of these substitutions is that none of the terms appearing in the momentum and diffusion equations are dependent on temperature and consequently these two equations may be solved simultaneously, but independently of the energy equation. Using this approach Baron obtains the velocity profiles, the concentration profiles and the skin-friction parameter, $c_f\sqrt{(u_e x/\nu_e C)}$, as a function only of the mass-transfer parameter $(\rho_w v_w)/\rho_e u_e)\sqrt{(u_e x/\nu_e C)}$. Any temperature effect is completely contained in the constant C.

The energy equation remains to be solved and, Baron reports that all the coefficients appearing in this equation were only mildly affected by temperature, allowing the assumption that all coefficients are functions *only* of concentration. This is a considerable simplification for now the energy equation is linear in temperature, since all coefficients are known functions of the dimensionless parameter, η, by virtue of the previously obtained solutions of the momentum

† This assumption is valid for hydrogen as well.

and diffusion equations.† As in the constant-property situation, the resulting energy equation, being linear, may be solved by first treating the non-dissipative case and then adding the adiabatic-wall solution. It follows that the low speed non-dissipative heat-transfer coefficients may be used for the high-speed case if the adiabatic-wall temperature replaces the free-stream temperature in the definition of the heat-transfer coefficient

$$q = h(T_r - T_w). \tag{19}$$

The recovery temperature, T_r, determined from the adiabatic-wall solution is reported in terms of a recovery factor, r, which for a given injected gas is a function only of the mass-transfer parameter $(\rho_w v_w/\rho_e u_e)\sqrt{(u_e x/\nu_e C)}$. In addition to the recovery factor, Baron also presents dimensionless heat-transfer coefficients for two binary systems, helium–air and carbon dioxide–air mixtures.

The second approach used by Baron is not as realistic as the above and will be mentioned only briefly. In this case he assumed that λ is a constant to be evaluated at wall condition and the following transformations are then applied to equations (2–8):

Approach 2:

$$\left.\begin{aligned} u &= \frac{\rho_e}{\rho}\frac{\partial\psi}{\partial y}, \quad v = -\frac{\rho_e}{\rho}\frac{\partial\psi}{\partial x} \\ \eta &= \frac{1}{2}\sqrt{\left(\frac{u_e}{\nu_e x C\lambda_w}\right)}\int_0^y \frac{\rho}{\rho_e}\,dy \\ \psi &= \sqrt{(\nu_e x u_e C\lambda_w)}\, f(\eta). \end{aligned}\right\} \tag{20}$$

Baron obtained some representative solutions for this simplified case and compared them with the more realistic case outlined above. This comparison is shown for helium injection on Fig. 9 and the agreement is only fair.

In a later publication [3] Baron generalizes his analysis to include the influence of pressure gradients. In addition, he presents a summary of his flat-plate results.‡

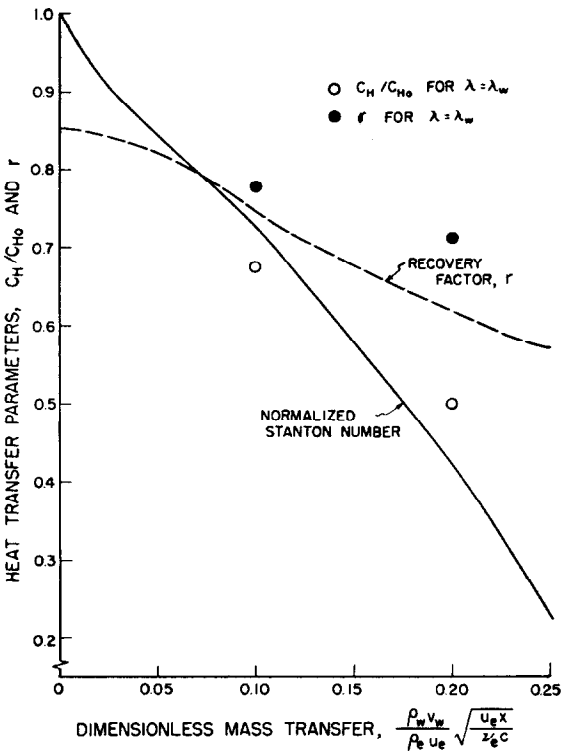

FIG. 9. Helium results of Baron.

Analysis of Eckert and co-workers [4–6]

Before attempting the complete binary problem including heat transfer, Eckert and Schneider first solved the isothermal case with hydrogen as the injected gas. The physical properties were allowed to vary with concentration and the methods outlined in Ref. 4 were used to calculate the variation. The resulting velocity distributions and skin friction are compared to the constant property results on Figs. 10 and 11. This comparison reveals that unstable S-shaped velocity profiles occur at relatively low values of the dimensionless mass transfer when compared

† There appears to be an error in Baron's final energy equation in Ref. 2. This results when he replaces u_e^2 by $(\gamma_e - 1)c_{p_2}M_e^2$ rather than the correct expression $(\gamma_e - 1)c_{p_e}M_e^2$. Consequently, the left hand side of Baron's energy equation 6:15, should be multiplied though by c_{p2}/c_{pe} to get the correct form.

‡ Care should be taken in using this reference since there is some confusion in nomenclature. The mathematical development utilizes a somewhat different transformation from that used by Baron in Ref. 2, although the figures are all shown in terms of the original variables of Ref. 2.

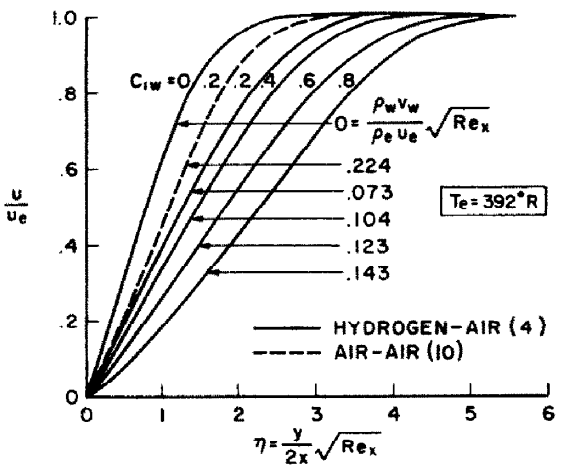

FIG. 10. Effect of light gas injection on laminar velocity profiles: isothermal case–flat plate.

with the constant property situation. The greater influence of a light gas on skin friction is obvious in Fig. 11, where at the same values of dimensionless mass transfer considerably lower skin friction occurs for the hydrogen injection. We, therefore, conclude that the light gas is more effective in reducing skin friction but on the other hand is more de-stabilizing to a laminar boundary layer.

In the analysis of the binary system including heat transfer, again using hydrogen as the mass-transfer medium, Eckert and his colleagues used the following transformation in dealing with equations (2–8).

$$\left.\begin{aligned} u &= \frac{\rho_e}{\rho}\frac{\partial \psi}{\partial y}, \quad v = -\frac{\rho_e}{\rho}\frac{\partial \psi}{\partial x} \\ \eta &= \frac{1}{2}\sqrt{\left(\frac{u_e}{\nu_e x}\right)}\int_0^y \frac{\mu_e}{\mu}\,dy \\ \psi &= \sqrt{(x u_e \nu_e)}\, f(\eta). \end{aligned}\right\} \quad (21)$$

The transformed equations were then solved using the best available property information for hydrogen–air mixtures. These exact solutions, which were obtained using an iterative procedure on an ERA 1103 electronic computer, are rigorously only valid for the specific conditions selected. (See Figs. 2 and 3.) An example of these results is shown in Fig. 12 where the dimensionless heat-transfer coefficients are shown for zero Mach number for two different wall-temperature conditions with the free stream at 392°R.

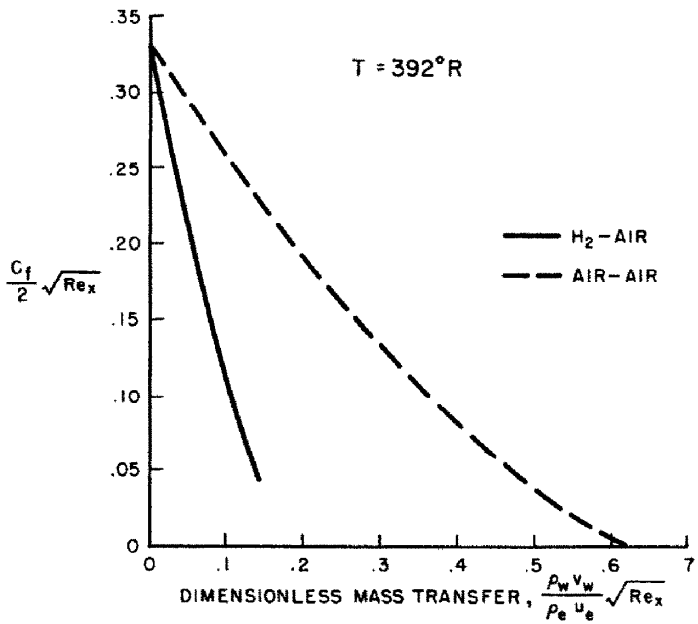

FIG. 11. Effect of light gas injection on skin friction: isothermal conditions–laminar flow: flat plate [4].

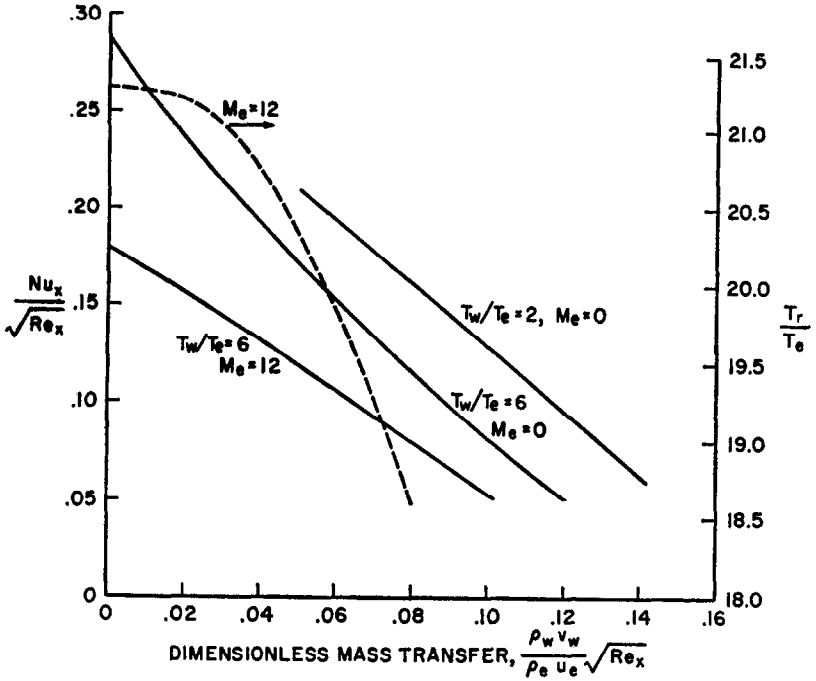

FIG. 12. Effect of hydrogen injection on laminar heat transfer: flat plate–T_e = 392°R. [5, 6].

Additionally, for Mach 12, the Nusselt number and recovery temperature, both of which must be known to determine the heat transfer, are shown for a set of specific conditions. In every case we find a considerable reduction in the heat transfer when only small amounts of hydrogen are transferred away from the wall into the boundary layer. The effectiveness of light-gas injection in decreasing the heat transfer in a high-speed boundary layer is obvious from this figure.

Analysis of Sziklas and Banas [7]

Sziklas and Banas report solutions for a number of different coolants: hydrogen, helium, water vapor, and air. In arriving at the final form of the energy equation they assumed that the specific heat ratio, γ, is the same for the injected coolant as for the main stream gas ($\gamma_1 = \gamma_2$). They then use the standard Blasius η— transformation essentially as given in equation (11). In obtaining their solutions the physical properties (including specific heat) were allowed to vary with both temperature and concentration. Methods of kinetic theory were used in the determination of these properties. As was the case with the results of Eckert, the results of Sziklas and Banas are applicable only to the specific conditions imposed in the analysis. Representative results for the helium study are given on Fig. 13, where, again, large reductions in heat transfer accompany small mass-transfer rates.

Analysis of Gross [8]

The isothermal laminar binary boundary layer on a flat plate was investigated by Gross [8] for three different injectant gases; hydrogen, carbon dioxide and iodine vapor. To obtain a solution of the governing equations (equations 2, 3 and 5), Gross used the standard Blasius transformation to arrive at a system of ordinary differential equations. These were then solved using a Runge–Kutta numerical method with the aid of a high-speed electronic computer.

The resulting values of the skin friction

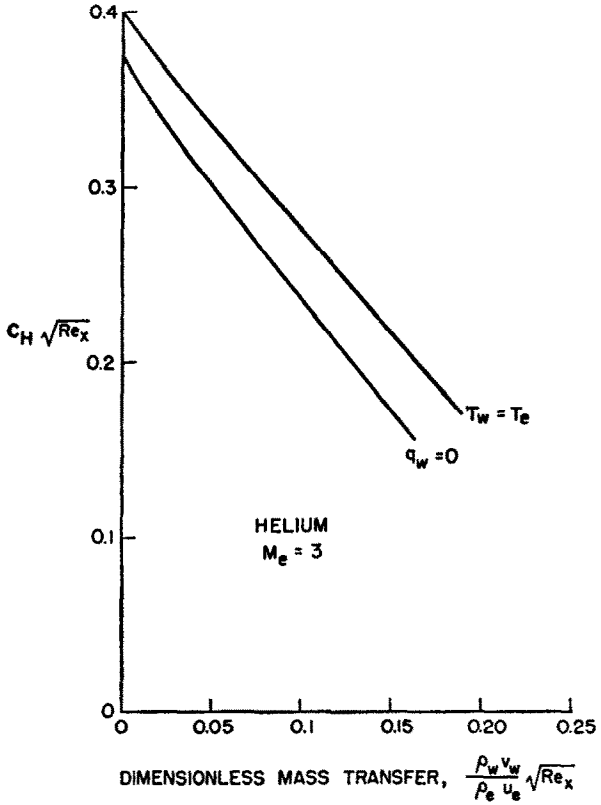

FIG. 13. Variation of laminar heat transfer with helium injection: Theory of Sziklas and Banas [7]. $T_e = 393°R$.

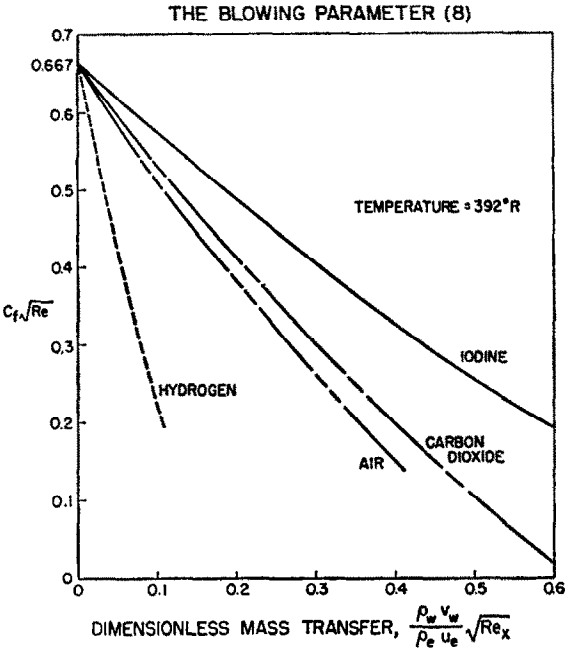

FIG. 14. Friction coefficient as a function of the blowing parameter [8].

coefficient for the three gases investigated are shown on Fig. 14. These results demonstrate that the addition of a heavy gas such as iodine vapor (molecular weight 253·8) is much less effective in reducing the skin friction coefficient than the lighter gases.

4. GENERALIZED PRESENTATION OF LAMINAR FLAT PLATE BINARY BOUNDARY LAYER RESULTS

It is our goal in this section to develop a generalized presentation which may be conveniently utilized by design engineers for predicting skin friction and heat transfer in the presence of mass-transfer cooling for laminar flow over surfaces with zero pressure gradient. The available analytical solutions briefly described above are used as the basis for the generalization. Since heat transfer and skin friction for solid surfaces in the absence of mass-transfer cooling can be calculated at the present time with a measure of confidence, the approach adopted here is to present the correction factors which must be applied to such solid wall calculations to account for the effect of mass addition. Thus the normalized skin-friction coefficient and heat transfer will be given as c_f/c_{f_0}, and q/q_0, respectively, where the subscript zero implies that the quantity is to be evaluated for the same free-stream and wall-temperature conditions neglecting the influence of mass transfer.

It was found that these normalized results for any one gas could be presented as a unique function of the mass-transfer parameter proposed by Baron, $(\rho_w v_w/\rho_e u_e)\sqrt{(u_e x/\nu_e C^*)}$, provided that the Chapman–Rubesin constant, C, was evaluated at the so-called reference temperature, T^*, given by equation (9). The success of this generalized presentation for skin friction is demonstrated in Figs. 15 and 16 which apply to hydrogen–air and helium–air binary systems, respectively. It appears that this representation

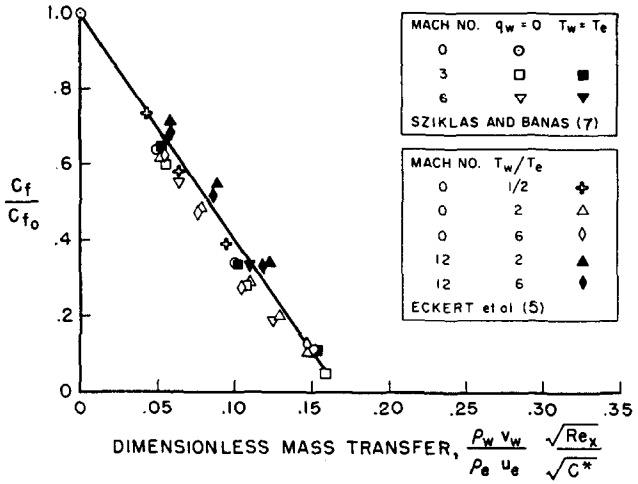

FIG. 15. Effect of mass transfer on skin friction: hydrogen-air: laminar flow-flat plate.

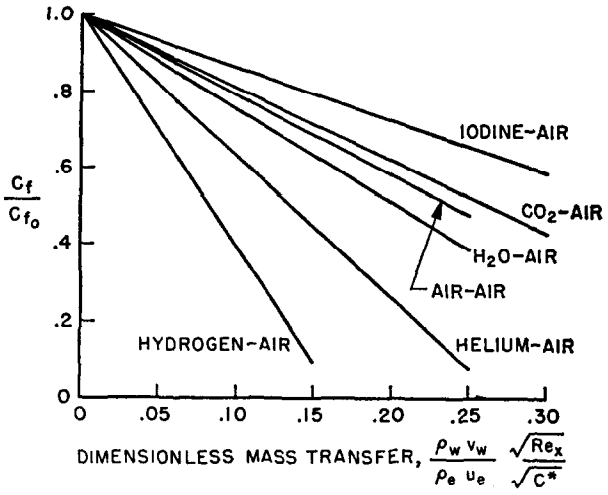

FIG. 17. Effect of mass transfer on skin friction: summary: laminar flow-flat plate.

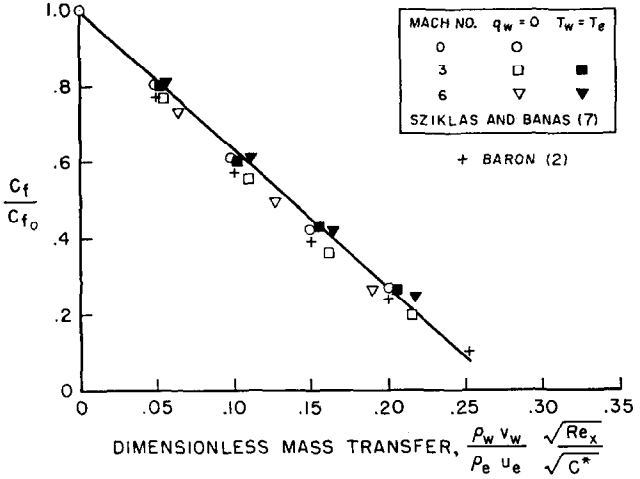

FIG. 16. Effect of mass transfer on skin friction: helium-air: laminar flow-flat plate.

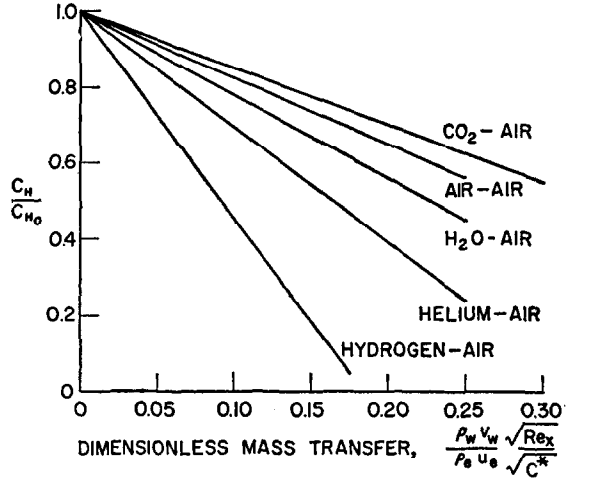

FIG. 18. Effect of mass transfer on Stanton number: laminar flow-flat plate.

is valid over a wide range of wall-temperature conditions and free-stream Mach numbers. This conclusion is true for the other binary systems as well and the reader is referred to the Appendix for verification of this conclusion. A summary of available skin-friction results for six gases is given on Fig. 17.

This same presentation was successful in correlating the normalized Stanton number, with the final results as shown on Fig. 18. Since the determination of the actual heat transfer requires the knowledge of the recovery factor as well as the Stanton number, the normalized recovery factor is shown on Fig. 19. It may be seen that some disagreement exists for the light-weight gases. Apparently the recovery factor is somewhat more sensitive to the different assumptions, particularly physical property variations, adopted by the various investigators. The effect on the final heat transfer prediction of this disagreement in recovery factor is reduced if the normalized heat transfer is directly considered

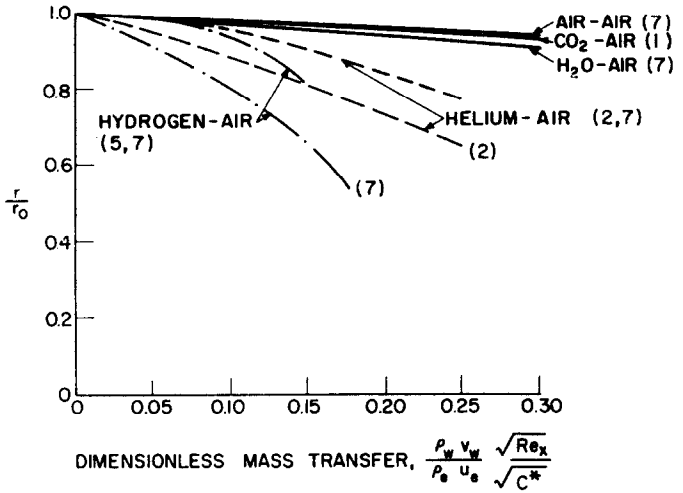

FIG. 19. Effect of mass transfer on recover factor: laminar flow–flat plate.

rather than the Stanton number. The resulting normalized heat transfer is shown on Figs. 20–22. It should be pointed out that some effect of the disagreement in recovery factor is still present in this presentation through the presence of C^*. However, for practical applications the wall temperature in general will be markedly lower than the recovery temperature; for this situation, inspection of the defining equation (9) for T^* reveals that any uncertainty in the recovery temperature has only a minor effect on the reference temperature itself, and consequently, only a minor effect on C^*.

It is apparent from Figs. 17 and 22 that the light gases are much more effective than the heavier gases in reducing heat transfer and skin friction. Inspection of these figures indicates that the normalized skin friction coefficient c_f/c_{f_0} and heat transfer q/q_0 vary linearly with the dimensionless mass-transfer parameter for all the gases shown. In particular, the results for air into air may be expressed by the following two equations.

$$q/q_0 = 1 - 1{\cdot}82\ \{(\rho_w v_w/\rho_e u_e)\ \sqrt{(Re_x/C^*)}\}$$

$$c_f/c_{f_0} = 1 - 2{\cdot}08\ \{(\rho_w v_w/\rho_e u_e)\ \sqrt{(Re_x/C^*)}\}.$$

It is of technical importance to determine whether the other gases can be made to agree with these equations by the simple expedient of multiplying the Baron dimensionless mass transfer parameter by a molecular weight ratio (m_2/m_1), raised to a constant exponent. This question can be answered by plotting the dimensionless mass transfer versus the molecular weight at a constant value of q/q_0 (or c_f/c_{f_0}). This is accomplished in Fig. 23 where it is seen that 1/3 represents a fair compromise for the value of the exponent although the very light gases as well as the heavier gases such as iodine show a significant departure. Recognizing that

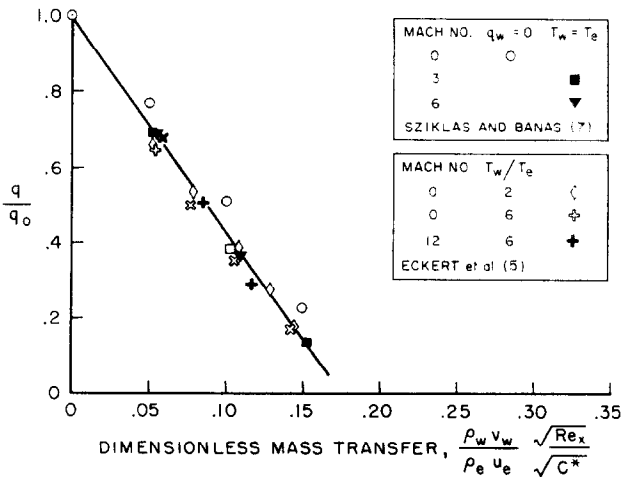

FIG. 20. Effect of mass transfer on heat transfer: hydrogen–air.

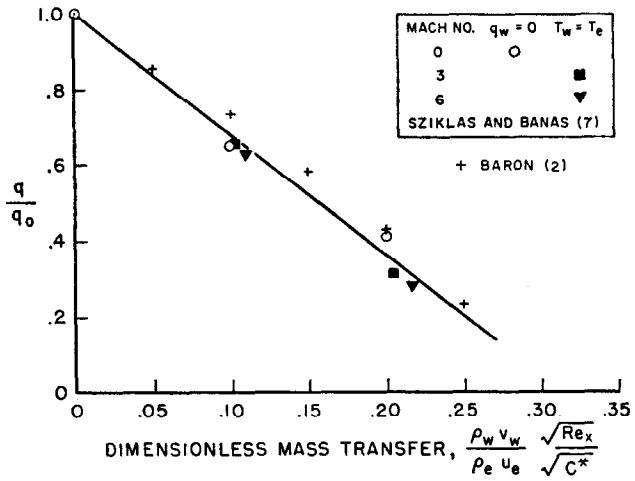

FIG. 21. Effect of mass transfer on heat transfer: helium–air.

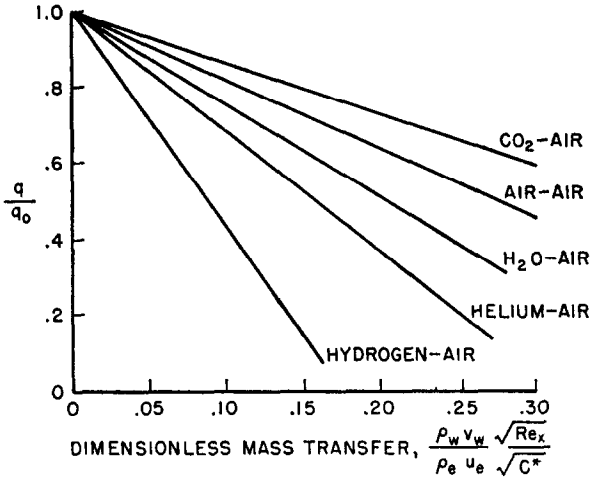

FIG. 22. Effect of mass transfer on heat transfer: summary.

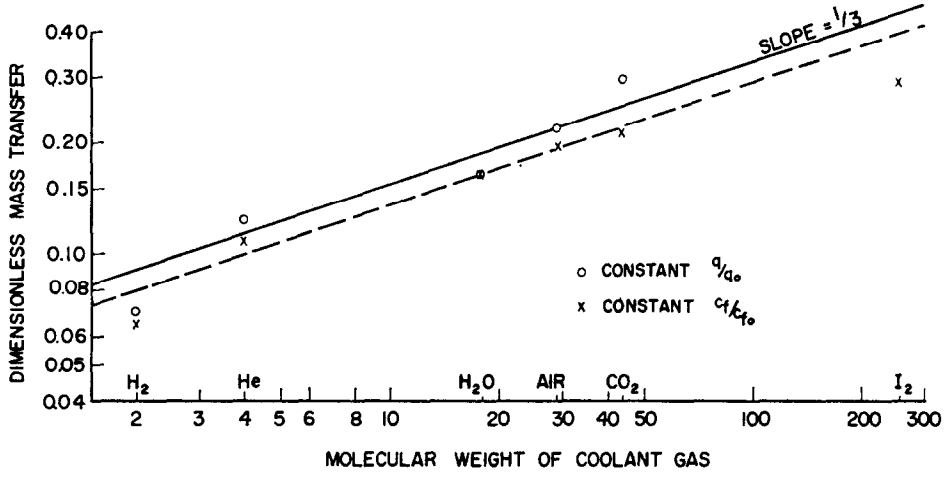

FIG. 23. Dimensionless mass transfer parameter versus molecular weight of coolant gas: laminar flow–flat plate.

such discrepancies do occur for the heavier and light gases, it nevertheless appears that the following equations represent the heat transfer and skin friction reasonably well.

$$\frac{q}{q_0} = 1 - 1{\cdot}82\,\{(m_2/m_1)^{1/3}(\rho_w v_w/\rho_e u_e)\sqrt{(Re_x/C^*)}\}$$

$$\frac{c_f}{c_{f_0}} = 1 - 2{\cdot}08\,\{(m_2/m_1)^{1/3}(\rho_w v_w/\rho_e u_e)\sqrt{(Re_x/C^*)}\}$$

It is recommended that these equations be used to predict the heat transfer and skin friction performance for mass-transfer cooling in a binary laminar boundary layer on a flat plate.

5. EFFECT OF PRESSURE GRADIENT ON LAMINAR MASS-TRANSFER COOLING

Up to the present time, little effort has been directed to the solution of the binary laminar

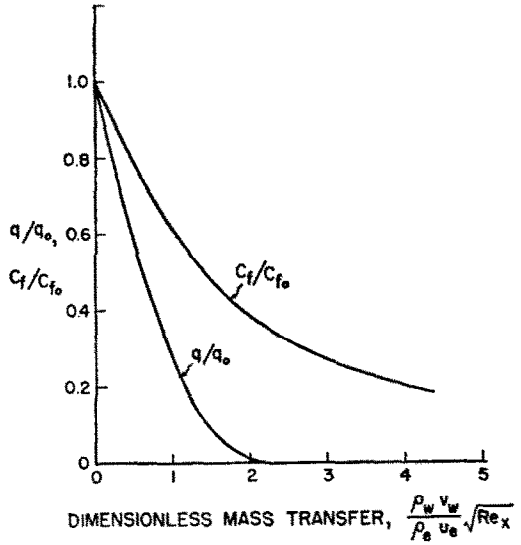

FIG. 24. Effect of air injection on heat transfer and skin friction coefficient: plane stagnation laminar flow [15] $Pr = 0{\cdot}7$.

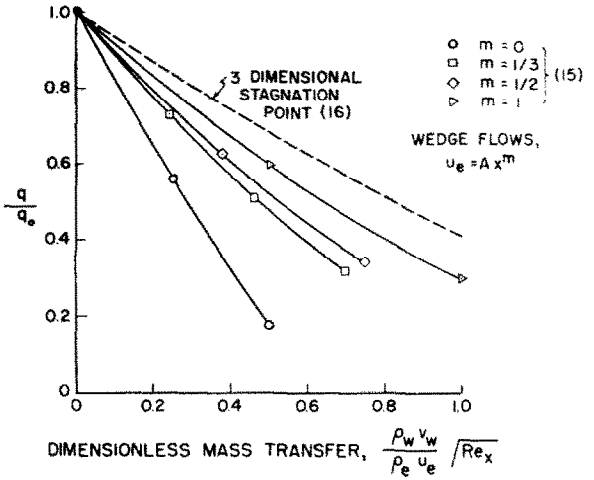

FIG. 25. Effect of pressure gradient on mass-transfer cooling: constant physical properties, $Pr = 0{\cdot}7$.

boundary-layer equations with finite pressure gradients. However, a measure of the influence of a pressure gradient on mass-transfer cooling can be obtained by returning to the constant-property boundary-layer model with normal injection (air-into-air) since solutions have been reported in this case for wedge-type pressure gradients (i.e. the free-stream velocity is described by $u_e = Ax^m$). Examination of these solutions [15] reveals that the presence of a favorable pressure gradient leads to more stable velocity profiles and, consequently, it appears that larger values of the dimensionless mass-transfer parameter, $(\rho_w v_w/\rho_e u_e)\sqrt{(Re_x)}$, may be obtained without causing transition to turbulence. Furthermore, the skin-friction coefficient remains finite in a favorable pressure gradient, with no apparent failure of the boundary-layer equations even for very large mass-transfer rates. However, the heat transfer does decrease to a diminishing value, with the thermal boundary layer displaced from the wall surface toward the free stream. An example of this skin-friction and heat-transfer behavior is given in Fig. 24 for the plane stagnation case ($m = 1$), and it may be seen that the heat transfer goes to zero at a value of the mass-transfer parameter of approximately 2 (as contrasted to 0·619 for the flat plate), while the skin friction is still approximately 40 per cent of its solid-wall value.

A direct comparison of the reduced heat flow, q/q_0, for four different pressure gradients ranging from the zero pressure gradient flat plate to the plane stagnation flow is given in Fig. 25. If a comparison is made at a fixed value of the dimensionless mass-transfer parameter, it is apparent that the greatest reduction in heat transfer occurs for the zero pressure gradient flat plate with the least reduction accompanying the plane stagnation flow. Therefore, to obtain a given reduction in heat flow, q/q_0, it is necessary to go to higher values of the dimensionless mass transfer as the pressure gradient increases. Since there exists considerable interest in the three-dimensional stagnation flow, Fig. 25 also presents the reduced heat transfer q/q_0 for air injection into such a region [16].

It finally remains to determine whether the relative position of the various coolant gases found for the flat plate geometry is markedly influenced by the presence of a pressure gradient. A recent analysis of Hayday [17] for hydrogen injection into a plane stagnation flow leads to the results shown in Fig. 26 and close inspection suggests that the molecular weight parameter found for the flat plate, i.e. $(m_2/m_1)^{1/3}$, is approximately valid for the plane stagnation flow.

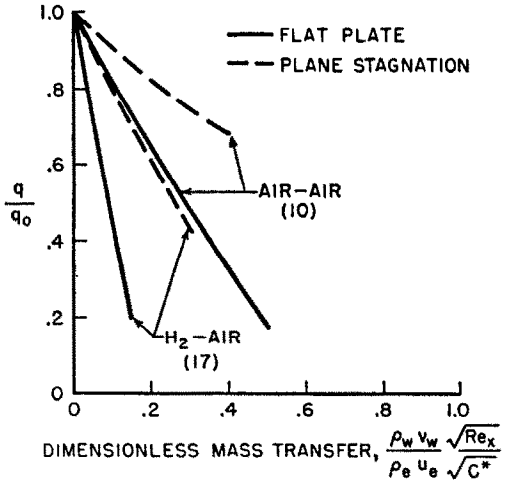

FIG. 26. Effect of pressure gradient on mass-transfer cooling.

As a result, it is suggested that air-into-air results be used to predict the effect of pressure gradient on laminar mass-transfer cooling; if a coolant other than air is transferred into the boundary layer the relative effectiveness of the various coolants is to be estimated from the flat-plate results. This is simply accomplished by using Fig. 25, changing the abscissa to read $[(\rho_w v_w/\rho_e u_e)\sqrt{(Re_x/C^*)}\,(m_2/m_1)^{1/3}]$.

REFERENCES

1. E. R. G. ECKERT, Mass transfer cooling, a means to protect high speed aircraft, presented at *First International Congress of Aeronautical Sciences*, Madrid, Spain, September 1958.
2. J. R. BARON, *The Binary Boundary Layer Associated with Mass Transfer Cooling at High Speed*. Mass. Inst. of Tech. Naval Supersonic Lab. Rpt. 160 (1956).
3. J. R. BARON, The hetrogeneous, laminar boundary layer. *RAND Symposium on Mass Transfer Cooling for Hypersonic Flight*.
4. E. R. G. ECKERT and P. J. SCHNEIDER, *Diffusion Effects in an Isothermal Binary Boundary Layer*. University of Minnesota, Heat Transfer Lab. Tech. Rpt. No. 5, November (1955).
5. E. R. G. ECKERT, P. J. SCHNEIDER, A. A. HAYDAY and R. M. LARSON, Mass transfer cooling of a laminar boundary layer by injection of a light-weight gas. *RAND Symposium on Mass Transfer Cooling for Hypersonic Flight*.
6. E. R. G. ECKERT, P. J. SCHNEIDER, A. A. HAYDAY and R. M. LARSON, Cooling of a laminar boundary layer by injection of a light-weight foreign gas. *Jet Propulsion*, **28**, 34 (1958).
7. E. A. SZIKLAS and C. M. BANAS, Mass transfer cooling in compressible laminar flow. *RAND Symposium on Mass Transfer Cooling for Hypersonic Flight*.
8. J. F. GROSS, *The Laminar Binary Boundary Layer*. RM-1915, The RAND Corporation, September (1956).
9. N. A. HALL, *Flow Equations for Multicomponent Fluid Systems*. University of Minnesota, Heat Transfer Lab. Tech. Rpt. No. 2, August (1955).
10. J. P. HARTNETT and E. R. G. ECKERT, Mass transfer cooling in a laminar boundary layer with constant fluid properties. *Trans. Amer. Soc. Mech. Engrs*, **79**, 247 (1957).
11. E. R. G. ECKERT, Engineering relations for heat transfer and skin friction in high-velocity laminar and turbulent boundary-layer flow over surfaces with constant pressure and temperature. *Trans. Amer. Soc. Mech. Engrs*, **78**, 1273 (1956).
12. M. ROMIG, Stagnation point heat transfer for hypersonic flow. *Jet Propulsion*, **26**, 1098 (1956).
13. D. R. CHAPMAN and M. W. RUBESIN, Temperature and velocity profiles in the compressible laminar boundary layer with arbitrary distribution of surface temperature. *J. Aero. Sci.* **19**, 341 (1947).
14. W. O. CARLSON and P. J. SCHNEIDER, *Transport Properties for Binary Gas Mixtures*. University of Minnesota, Heat Transfer Lab. Tech. Rpt. No. 7, January (1956).
15. W. B. BROWN and P. L. DONOUGHE, *Tables of Exact Laminar Boundary-Layer Solutions when the Wall is Porous and Fluid Properties are Variable*. Nat. Advisory Comm. Aeronaut. Tech. Note 2479, September (1951).
16. E. RESHOTKO and C. B. COHEN, *Heat Transfer at the Forward Stagnation Point of Blunt Bodies*. Nat. Advisory Comm. Aeronaut. Tech. Note 3513, July (1955).
17. A. A. HAYDAY, *Mass Transfer Cooling in a Laminar Boundary Layer in Steady Two-Dimensional Stagnation Flow*. University of Minnesota, Heat Transfer Lab. Tech. Rpt. No. 19, April (1958).

APPENDIX A

Additional verification of the dimensionless presentations

In this section the reduced skin friction c_f/c_{f_0} and heat transfer q/q_0 are plotted as functions of the mass-transfer parameter for all of the injected materials. (Figs. 27 and 28.) It may be seen that the summary curve given in the main body of the report accurately represents the calculated performance.

Furthermore, the Stanton number and recovery factors are given in detail. (Figs. 29–32.) In the latter case, it is apparent that discrepancies exist in the case of hydrogen–air and helium–air,

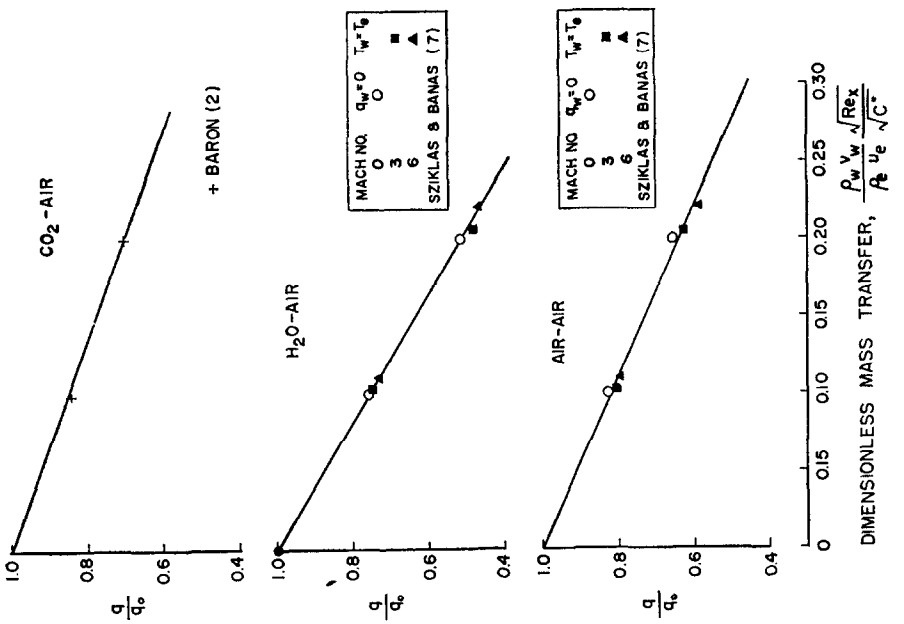

FIG. 28. Effect of mass transfer on heat transfer.

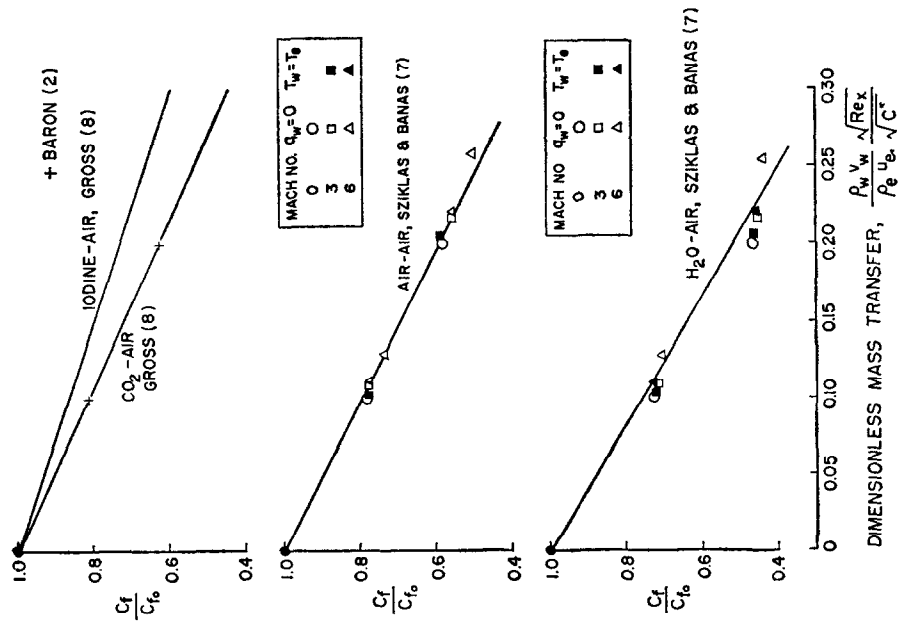

FIG. 27. Effect of mass transfer on skin friction: laminar flow–flat plate.

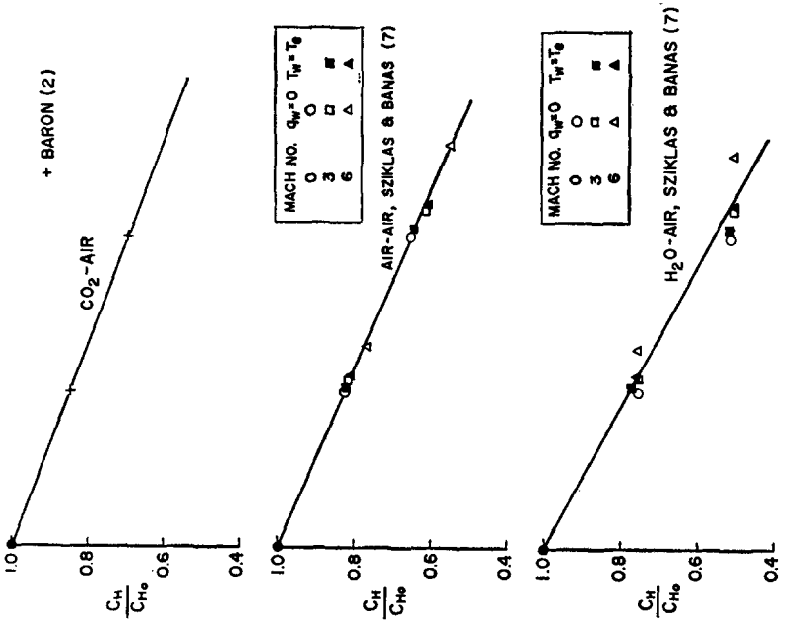

FIG. 30. Effect of mass transfer on Stanton number: laminar flow-flat plate.

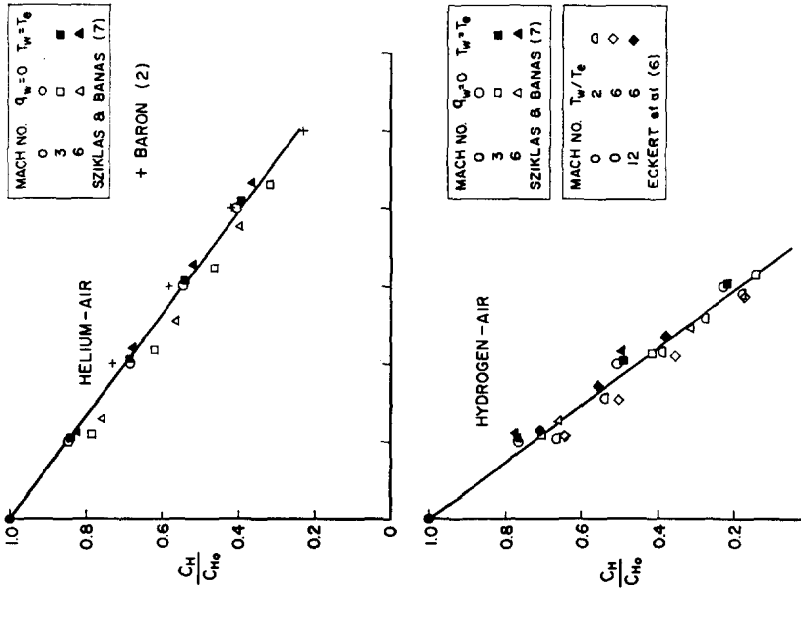

FIG. 29. Effect of mass transfer on Stanton number: laminar flow-flat plate.

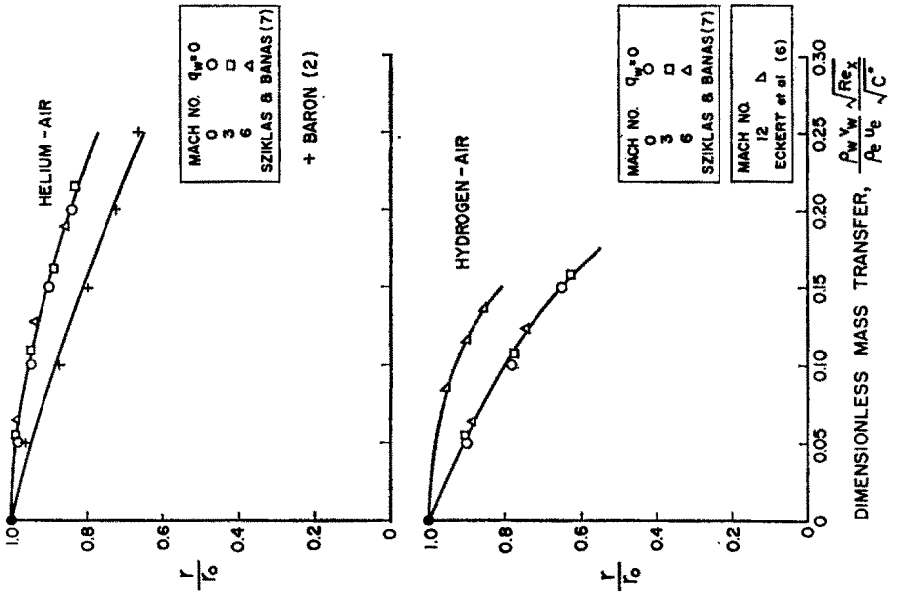

FIG. 32. Effect of mass transfer on recovery factor: laminar flow–flat plate.

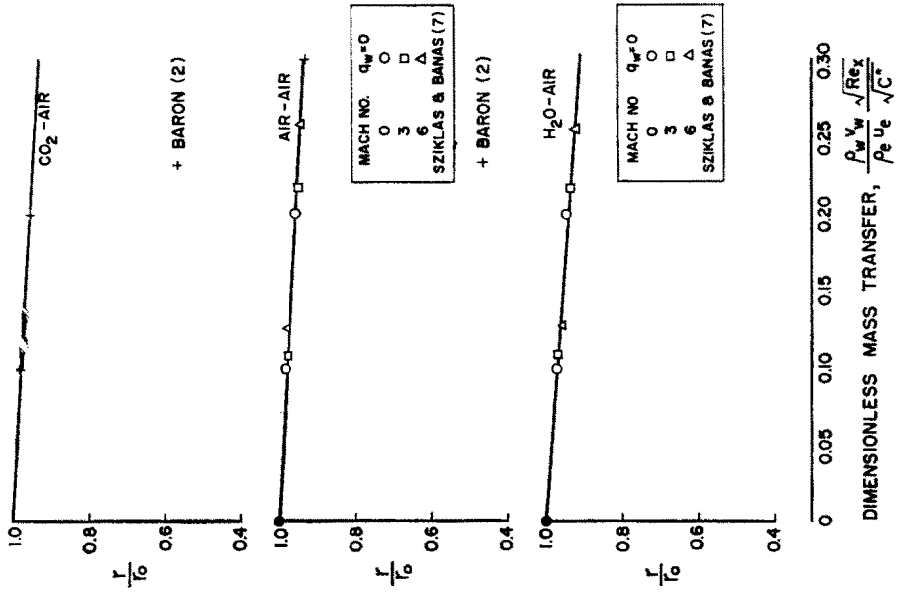

FIG. 31. Effect of mass transfer on recovery factor: laminar flow–flat plate.

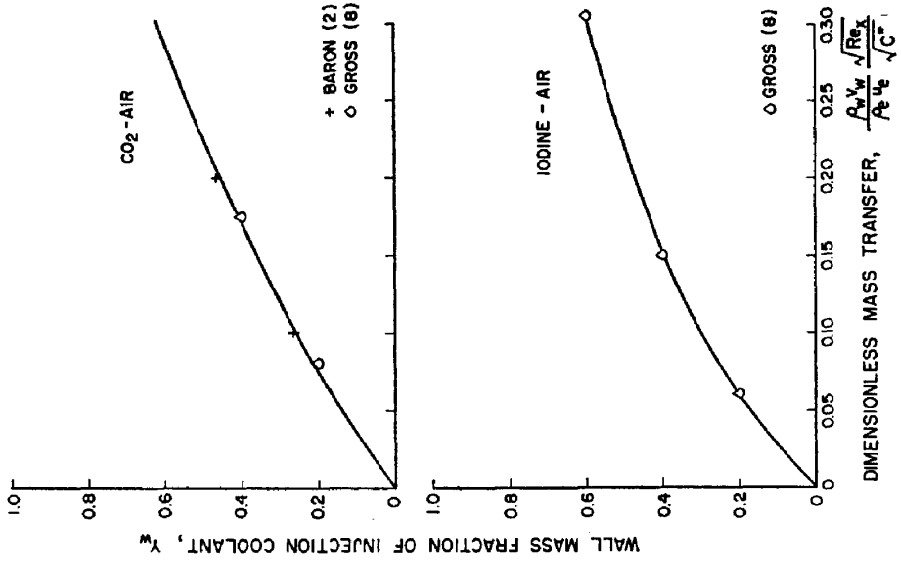

FIG. 34. Wall mass fraction versus dimensionless mass transfer.

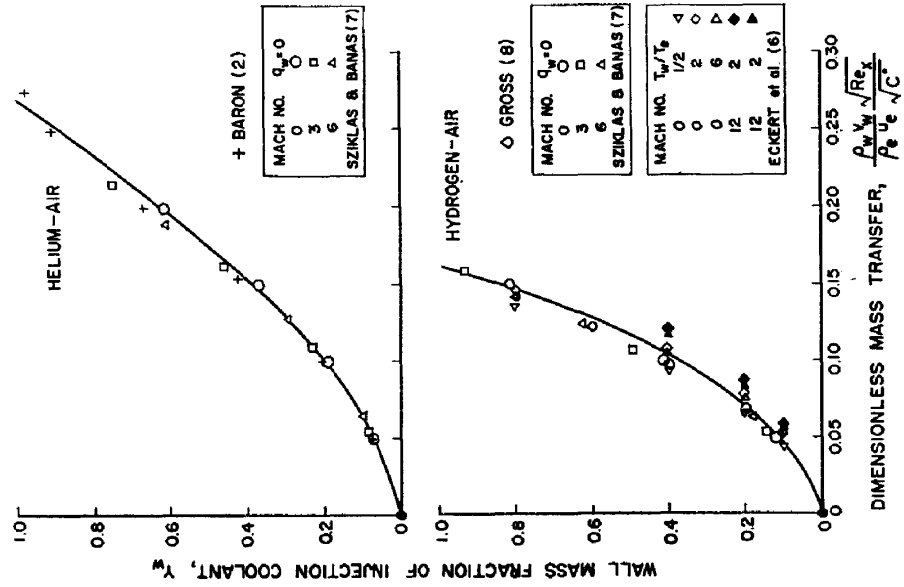

FIG. 33. Wall mass fraction versus dimensionless mass transfer.

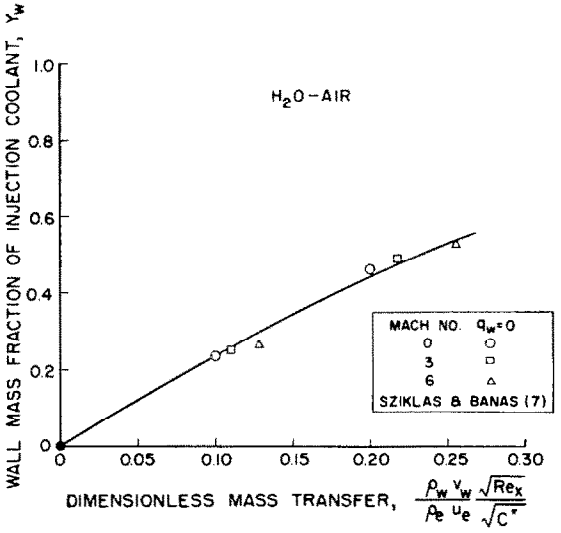

FIG. 35. Wall mass fraction versus dimensionless mass transfer.

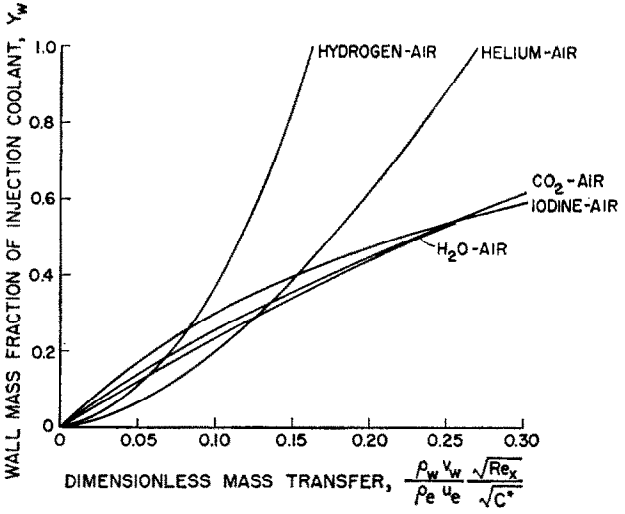

FIG. 36. Wall mass fraction versus dimensionless mass transfer: summary.

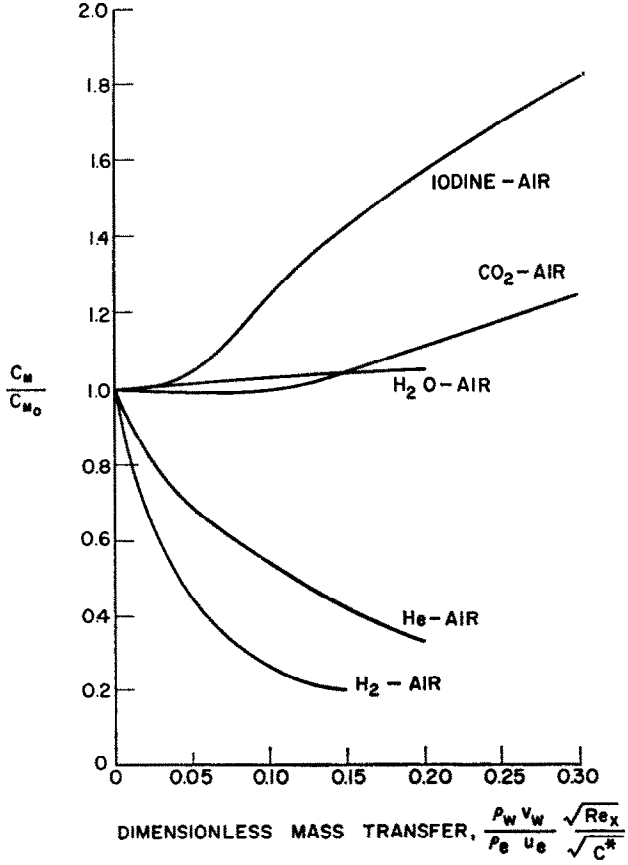

FIG. 37. Effect of mass-transfer rate on the mass transfer Stanton number.

probably due to the uncertainty in the physical property values under such extreme temperature conditions.

APPENDIX B

Relation between wall concentration and mass transfer parameter

In the treatment of a subliming surface, it is important to know the relationship between the wall mass fraction and the dimensionless mass-transfer rate. A generalized presentation of the wall mass fraction for each gas appears possible with the aid of the Baron variable $(\rho_w v_w/\rho_e u_e)\sqrt{(Re_x/C^*)}$ and these are shown for some five gases in Figs. 33–36. A summarizing curve is also available in Fig. 36.

APPENDIX C

On the use of mass transfer results for prediction of heat transfer

It is rather common practice to experimentally obtain mass transfer Stanton numbers, c_M, using materials which sublime or evaporate, such as naphthalene or water, and to interpret these results directly as solid wall heat transfer Stanton number, c_{H_0} (in some instances a correction factor involving the Lewis number is applied). However, considerable caution must be exercised in this procedure as is obvious from a comparison of Fig. 37 with Fig. 18 of the main text. Fig. 18 shows the heat transfer Stanton numbers in the form of c_H/c_{H_0}, where c_H is the heat transfer Stanton number in the presence of mass transfer, while c_{H_0} is the Stanton number for a solid wall exposed to the same free stream conditions (i.e. c_{H_0} is the limiting value of c_H as the mass-transfer rate goes to zero). Fig. 37 is a similar curve for the mass transfer Stanton number, c_M, again normalized with respect to the value at the zero mass-transfer condition. For water vapor–air and CO_2–air mixtures the limiting Stanton values, c_{H_0} and c_{M_0}, are in good agreement (i.e. $c_{H_0} = c_{M_0}$) and since c_M/c_{M_0} does not depart appreciably from unity over a range of mass-transfer rates, it would appear that the measured mass transfer Stanton number, c_M, for these two systems could indeed be interpreted as solid wall heat transfer Stanton number, c_{H_0}. However, for the other gas mixtures, it must be concluded that considerable error would arise in the use of this procedure.